

THE ALBEDO–COLOR DIVERSITY OF TRANSNEPTUNIAN OBJECTS

PEDRO LACERDA¹, SONIA FORNASIER², EMMANUEL LELLOUCH², CSABA KISS³, ESA VILENIUS⁴, PABLO SANTOS-SANZ⁵,
MIRIAM RENGEL¹, THOMAS MÜLLER⁴, JOHN STANSBERRY⁶, RENÉ DUFFARD⁵, AUDREY DELSANTI^{2,7},
AND AURÉLIE GUILBERT-LEPOUTRE⁸

¹ Max-Planck-Institut für Sonnensystemforschung, Justus-von-Liebig-Weg 3, D-37077 Göttingen, Germany

² LESIA-Observatoire de Paris, CNRS, UPMC, Université Paris-Diderot, 5 place Jules Janssen, F-92195 Meudon, France

³ Konkoly Observatory, MTA CSFK, 1121 Budapest, Konkoly Th. M. út 15-17, Hungary

⁴ Max-Planck-Institut für Extraterrestrische Physik, Postfach 1312, Giessenbachstrasse, D-85741 Garching, Germany

⁵ Instituto de Astrofísica de Andalucía (IAA-CSIC), Glorieta de la Astronomía, s/n. E-18008 Granada, Spain

⁶ Space Telescope Science Institute, 3700 San Martin Drive, Baltimore, MD 21218, USA

⁷ Aix Marseille Université, CNRS, Laboratoire d'Astrophysique de Marseille (LAM), UMR 7326, F-13388 Marseille, France

⁸ European Space Agency/ESTEC, Keplerlaan 1, 2201-AZ Noordwijk, Netherlands

Received 2014 June 4; accepted 2014 August 12; published 2014 August 29

ABSTRACT

We analyze albedo data obtained using the *Herschel Space Observatory* that reveal the existence of two distinct types of surface among mid-sized trans-Neptunian objects. A color–albedo diagram shows two large clusters of objects, one redder and higher albedo and another darker and more neutrally colored. Crucially, all objects in our sample located in dynamically stable orbits within the classical Kuiper Belt region and beyond are confined to the bright red group, implying a compositional link. Those objects are believed to have formed further from the Sun than the dark neutral bodies. This color–albedo separation is evidence for a compositional discontinuity in the young solar system.

Key word: Kuiper belt: general

Online-only material: color figures

1. INTRODUCTION

In the current paradigm, developed largely to explain the orbits of trans-Neptunian objects (TNOs), the dynamical architecture of the solar system is thought to have evolved considerably since formation, particularly in the first billion years (Tsiganis et al. 2005). A violent planetary instability involving Jupiter and Saturn is hypothesized to have caused Uranus and Neptune to migrate from their formation region (within 15 AU) to their current orbits. This event led to the stochastic dispersal of the planetesimal disk and resulted in bodies formed at various distances from the Sun being stored together in the trans-Neptunian space (Levison et al. 2008). This dynamical restructuring may explain the broad diversity seen in the properties of TNOs, but could also obscure links with birth location that carry information about the properties of the protoplanetary disk. One exception is the cold classical population (Figure 1), which stands out as possessing a number of properties that suggest a unique origin and evolution (Gladman et al. 2008). Cold classicals have low inclination orbits in the region known as the classical Kuiper Belt, a donut-shaped structure located between the 3:2 and the 2:1 Neptunian mean-motion resonances (MMRs) at 39 and 47 AU. Dynamically, these objects show no signs of past interactions with Neptune: they are decoupled from the ice giant and are stable on gigayear timescales (Batygin et al. 2011). Physically, when compared to other TNOs, cold classicals possess redder surfaces (Tegler & Romanishin 2000), smaller sizes (Levison & Stern 2001), and a much larger abundance of binaries (Stephens & Noll 2006), including weakly bound pairs that would have been disrupted by encounters with planets (Parker & Kavelaars 2010). Attempts to explain the origin of this population closer the Sun and their transport out to the classical Kuiper Belt following the planetary instability have been unsuccessful (Levison & Morbidelli 2003; Levison et al. 2008, but see Morbidelli et al. 2014).

Consequently, cold classicals are most simply understood as survivors of an original population that formed in-situ (Levison & Stern 2001; Batygin et al. 2011) and, as such, are representative of the properties of bodies that originally formed beyond Neptune. In this Letter, we analyze albedo data for 109 TNOs and Centaurs obtained using the *Herschel Space Observatory* and find that cold classical TNOs are not as unique in terms of their surface properties as previously believed. Indeed, all sampled TNOs in dynamical classes thought to originate beyond Neptune display similar color/albedo properties.

2. *HERSCHEL* “TNOs ARE COOL” SURVEY AND SAMPLE

Herschel was the first large aperture (3.5 m) space telescope to operate in the far-infrared and submillimeter and it offered a unique chance to measure the thermal radiation from the cool TNOs (equilibrium temperatures ~ 40 K). Starting in 2009, we conducted the “TNOs Are Cool” survey of the outer solar system using *Herschel* to measure albedos and sizes for 130 TNOs and Centaurs (Müller et al. 2009), tripling the size of the existing sample. Thermal observations obtained earlier using the *Spitzer Space Telescope* (Stansberry et al. 2008) were used to complement the *Herschel* data, and a handful of objects in our sample have independent, highly accurate diameter (and albedo) estimates from stellar occultations. The thermal data were combined with existing optical data to derive albedos and diameters using the radiometric method or more detailed thermophysical models when justified. Details of the survey and modeling of albedos and diameters have been published in the “TNOs Are Cool” series of papers (e.g., Müller et al. 2010; Lellouch et al. 2010, 2013; Lim et al. 2010; Santos-Sanz et al. 2012; Mommert et al. 2012; Vilenius et al. 2012, 2014; Pál et al. 2012; Fornasier et al. 2013; Kiss et al. 2013, and C. Kiss et al. in preparation).

Table 1
TNO/Centaur Sample Properties

Dynamical class	N	Albedo		Color	Surface Types
		Median	$CI_{68\%}$		
Scattered disk	9	0.05	(0.04, 0.09)	16.3 ± 12.6	DN, BR
Centaur	22	0.06	(0.04, 0.13)	21.5 ± 16.5	DN, BR
Hot classical	25	0.08	(0.04, 0.13)	22.8 ± 15.6	DN, BR
Plutinos	20	0.09	(0.05, 0.16)	20.1 ± 15.4	DN, BR
Inner classical	4	0.09	(0.06, 0.18)	22.4 ± 12.8	DN, BR
Middle resonant	1	0.12	(0.08, 0.17)	28.2	BR
Outer resonant	12	0.13	(0.08, 0.22)	31.6 ± 12.8	BR
Cold classical	8	0.15	(0.09, 0.23)	33.2 ± 10.3	BR
Detached TNOs	8	0.17	(0.08, 0.37)	33.2 ± 14.6	BR

Notes. Columns are (1) dynamical class, (2) number of TNOs, (3) median albedo and 68% confidence interval, (4) mean spectral slope in $\%/ (1000 \text{ \AA})$ and standard deviation. The statistics include measurement uncertainties by bootstrap resampling and excludes dwarf planets and Haumea-type TNOs. (5) Dominant surface types present in class (see the caption for Figure 1).

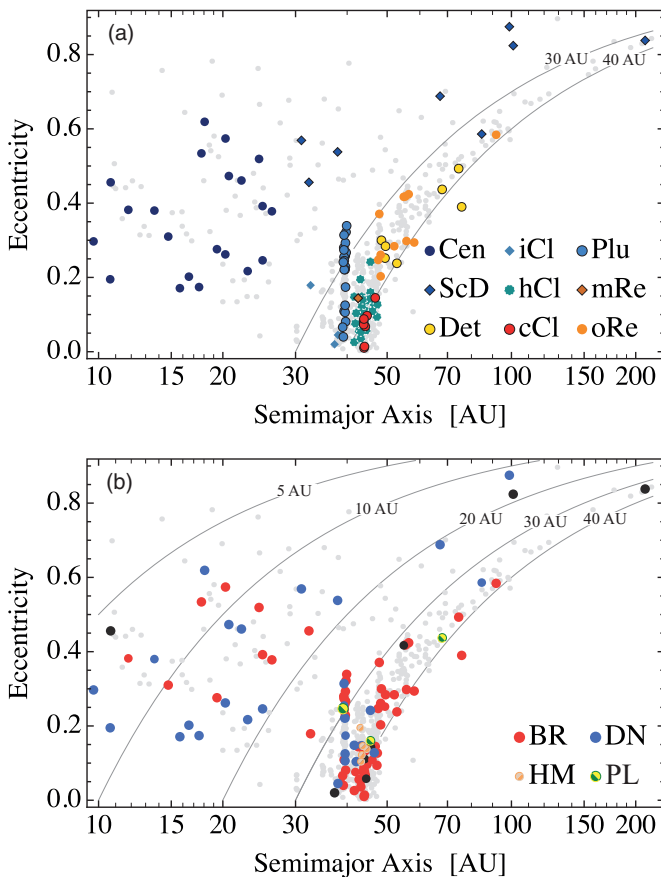


Figure 1. (a) Orbital distribution (semimajor axis vs. eccentricity) of our sample (Cen = Centaurs, iCl = inner classicals, Plu = Plutinos, ScD = scattered disk, hCl = hot classicals, mRe = middle resonants, Det = detached, cCl = cold classicals, oRe = outer resonants). The light gray points mark TNOs not observed by *Herschel*. The curves of constant perihelion are plotted in solid gray and labeled. (b) Same as panel (a), but color-coded by surface type (BR = bright red, DN = dark neutral, HM = Haumea-type, PL = dwarf planets, black points have large uncertainties and ambiguous surface type.)

(A color version of this figure is available in the online journal.)

Our sample covers the different dynamical classes to enable comparative studies. We adopt a widely accepted dynamical classification scheme (Gladman et al. 2008) that groups TNOs into resonant, scattered, detached, classical (Figure 1; Table 1). We split the classicals into hot and cold at orbital inclination $i = 5^\circ$, and the resonants into inner (objects in the 3:2 MMR

and in resonances closer to the Sun), middle (located between the 3:2 MMR and the 2:1 MMR), and outer (2:1 MMR and beyond). In our data, the inner resonants are represented by 21 Plutinos (3:2 MMR), the middle resonants consist of a single TNO (5:3 MMR), and the outer resonants include 4 TNOs in the 2:1 MMR, 1 in the 9:4, 4 in the 5:2, 1 in the 8:3 and 1 in the 11:2. Our sample also includes 4 inner classicals, which lie just sunward of the 3:2 MMR, and 22 Centaurs, which represent an intermediate dynamical stage between TNOs and Jupiter family comets (JFCs; Volk & Malhotra 2008).

3. RESULTS

The *Herschel* albedos (geometric, V band) are shown in Figure 2, plotted against visible color quantified by the spectral slope, S' , in units of $\%/ (1000 \text{ \AA})$ (Luu & Jewitt 1990). Spectral slopes are measured directly from optical spectra when available (Fornasier et al. 2009) or derived from broadband BR photometry (Jewitt 2002) taken from the literature (Hainaut et al. 2012; Peixinho et al. 2012; Perna et al. 2013). In the remaining text, we refer to the spectral slopes simply as “color.” We plot only those 109 objects for which both albedo and color are known. The TNOs are broadly split into two clusters: a dark neutral clump of objects with low albedos and shallow spectral slopes ($p_V \sim 0.05$, $S' \sim 10\%$), and a bright red agglomeration with higher albedos and significantly redder slopes ($p_V \sim 0.15$, $S' \sim 35\%$). These two surface types encompass $>90\%$ of all mid-sized TNOs in our sample. A smaller cluster of bright neutral objects includes the dwarf planets Eris, Pluto, and Makemake which have characteristic ultra-high albedos, plus Haumea and another four objects with Haumea-type surfaces.

The orbital distribution of bright red and dark neutral objects is shown in Figure 1 and shows that TNOs with both surface types exist scattered throughout the entire trans-Neptunian region with no obvious trend in mean heliocentric distance or closest approach to the Sun. We take this to indicate that the surface types are unlikely to be set by current conditions (temperature, irradiation) that depend on the object’s distance to the Sun and are probably primitive. Figure 3 shows how TNOs in different dynamical classes are distributed in the color–albedo diagram. Interestingly, while some dynamical families have objects in both surface-type clusters, others are exclusively composed of bright red objects. The latter include the cold classicals, the middle and outer resonants, and the detached TNOs.

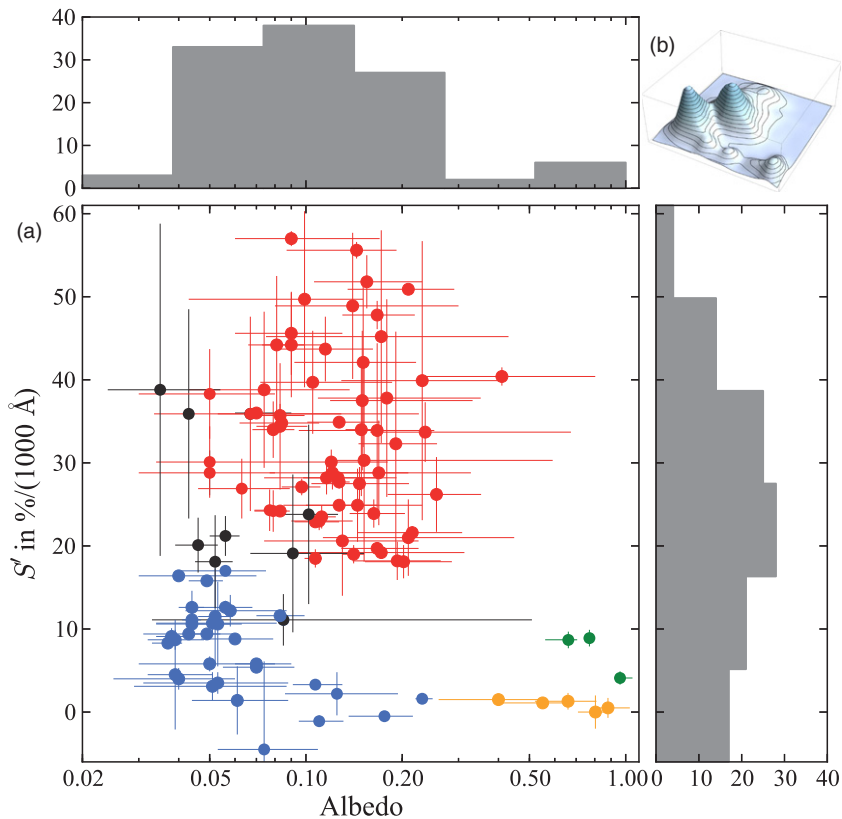


Figure 2. (a) Color–albedo diagram for 109 TNOs showing two main clusters, one composed of dark neutral objects (blue points, albedos ~ 0.05 and $S' \sim 10\%$), and another of bright red objects (red points, albedo ~ 0.15 and $S' \sim 30\%$). The black points have large uncertainties and ambiguous surface type. Large TNOs (green) and objects with Haumea-type surfaces (orange) occupy a third group (bottom right). Albedo/color histograms are shown in gray. (b) Smooth 2D histogram (Gaussian kernel, width 3% of full ranges, weighted by errorbars) of the color–albedo distribution shown in panel (a).

(A color version of this figure is available in the online journal.)

The two main surface-type clusters in Figure 2 were identified automatically using the *Mathematica 9* procedure `FindClusters[]`,⁹ which we set to implement an agglomerative algorithm, using the Euclidean distance function. Eris, Pluto, Makemake, and objects with Haumea-type surfaces were excluded, leaving a set of $N = 101$ TNOs. As seen in Figure 2, the bulk of the TNOs falls consistently in one of the two groups, with only a few objects near the gap between clusters having ambiguous classification due to their large uncertainties. To assess the significance of the two clusters, we employed three methods. First, we randomly generated 1000 sets of points in the unit square, each equal in size to the original data. We found two clusters in 1.3% of the random sets, three clusters in 0.1%, and four clusters in 0.1% of the cases, with the remaining 98.5% of random sets being deemed unclustered. Second, we used the gap statistic (Tibshirani et al. 2001) to quantify how often is a reference distribution that better represents the data (generated along the principal components of the data as opposed to randomly in a square) as strongly clustered as the original. The technique selected 2 clusters as the optimal number in our data and found that the same was true for 14 out of 1000 (1.4%) replications of the data drawn from the optimized reference distribution; the remaining 987 cases were considered unclustered. Finally, we employed the bootstrapping technique described in Efron & Tibshirani (1993). Here, smooth null distributions from which bootstrap replications can be drawn are generated by convolving the normalized data with a two-dimensional (2D) Gaussian of

width w . The number of maxima of the convolved distribution corresponds to the number of clusters in that particular bootstrap replication. The value w is selected to be the smallest that produces a unimodal null distribution from the data. In 1000 bootstrap replications (each with $N = 101$) drawn from the null distribution, the fraction found to have two or more clusters was $p = 0.008$. Thus, all three methods find a low probability ($\sim 1\%$) that the clustering seen in the data is random.

4. DISCUSSION

We find that the surfaces of most TNOs fall into one of two main types: bright red, or dark neutral (Figure 2). Furthermore, while some dynamical classes have both types of objects, others have only bright red TNOs. The latter are those that probably originated far from the Sun, so their characteristic surfaces would be representative of outer solar system planetesimals. As discussed above, cold classicals likely formed in-situ and have remained unperturbed dynamically (Batygin et al. 2011). Detached TNOs are currently decoupled from Neptune, and some have been claimed to be part of the inner Oort Cloud (Trujillo & Sheppard 2014). While the origin of these objects is unknown, most scenarios suggest that they formed beyond Neptune (Gladman et al. 2002). Middle and outer resonants may have been swept from closer to the Sun during Neptune’s migration. In the classic resonance sweeping scenario (Malhotra 1995), TNOs currently in the $p:q$ MMR originated in the region $a_N(p/q)^{2/3} < a < 30(p/q)^{2/3}$, where a_N is the starting point of Neptune’s migration in AU. Assuming that Neptune began its outward migration at ~ 20 AU

⁹ <http://reference.wolfram.com/mathematica/tutorial/PartitioningDataIntoClusters.html>

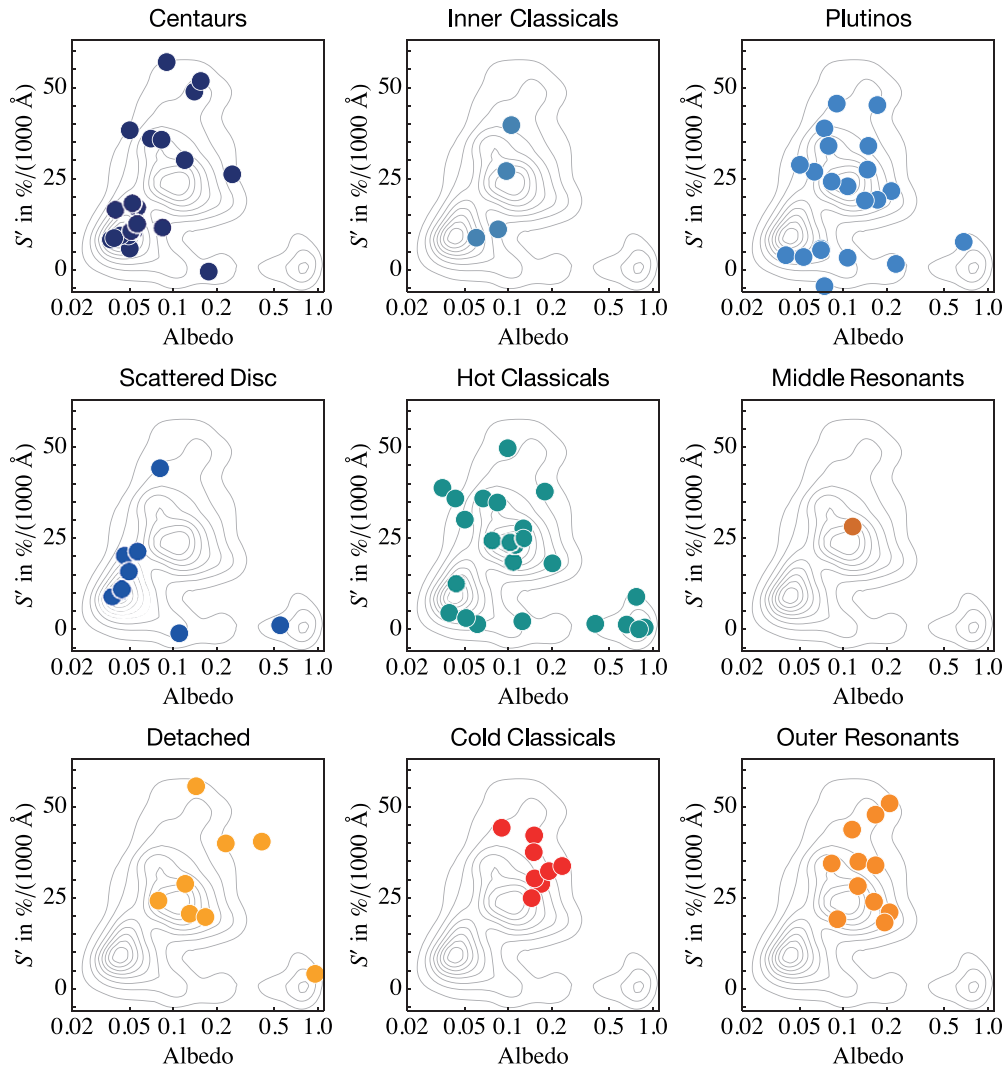


Figure 3. Same as Figure 1 with objects gathered by dynamical class. Underlying contours are a density map of all objects obtained by bootstrap-sampling each object 100 times assuming its albedo (color) follows a lognormal (normal) distribution set by the observing uncertainties.

(A color version of this figure is available in the online journal.)

(Malhotra 1995), the 2:1 MMR, the innermost of the outer resonances, includes objects captured at 32 AU and beyond. The alternative mechanism to populate the MMRs invokes chaotic resonant capture during the circularization of Neptune’s orbit following the planetary instability phase (Levison et al. 2008). An initially eccentric Neptune would produce a chaotic sea of wide, overlapping MMRs in the trans-Neptunian region. As the planet’s orbit circularized, the MMRs narrowed and retained in-situ planetesimals that happened to be at resonant locations. In summary, in the resonance sweeping scenario the middle and outer resonants are likely dominated by objects formed beyond ~ 30 AU, but in the chaotic capture mechanism it is possible that they include objects formed closer to the Sun.

In contrast, Plutinos, scattered TNOs, inner and hot classicals, and Centaurs, which are believed in most dynamic evolution models to contain remnant planetesimals formed over a wider range of heliocentric distances, from about 20 AU out to the current classical Kuiper Belt (Petit et al. 2011), include a mixture of bright red and dark neutral objects. This is consistent with previous findings that different, dynamically excited TNO populations are composed of two main types of surfaces (Fraser & Brown 2012; Bauer et al. 2013). In the classic sweeping

resonance scenario the Plutinos were captured from ~ 26 AU outward, while the scattered disk (Morbidelli et al. 2004) and the hot classicals (Gomes 2003) include several objects formed at 20–30 AU and scattered following the planetary instability event and Neptune’s migration through the disk. The origin of the inner classicals is uncertain, but they may be an extension of the hot classical component (Kavelaars et al. 2009), while the Centaurs probably originate in one of the populations above (Volk & Malhotra 2008) and are expected to be physically similar.

Previous attempts to find trends in the surface properties of TNOs have relied mostly on broadband colors. Three key findings emerged from the analysis of colors: that TNOs have the most diverse surfaces of all small bodies in the solar system (Luu & Jewitt 1996), that low eccentricity and inclination objects in the classical Kuiper Belt possess significantly redder surfaces (Tegler & Romanishin 2000)—these objects are now recognized as the cold classical population—and that Centaurs and small, excited TNOs are a mixture of neutrally colored and very red objects, with no intermediate colors (Peixinho et al. 2003, 2012; Fraser & Brown 2012; Fraser et al. 2014). The mixture of neutral and red objects in these populations is taken

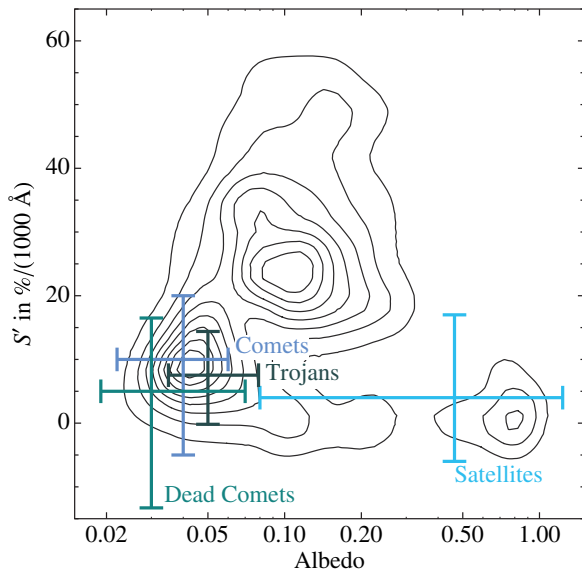


Figure 4. Albedo and color ranges (central 95%) for small body populations in the inner/intermediate solar system superimposed on TNO data contours (Figure 3). Comet data include Jupiter family and Oort Cloud comets. Jovian L4 and L5 Trojans are included, and satellites of the giant planets.

(A color version of this figure is available in the online journal.)

to mean that they include planetesimals formed at two different locations in the disk, as opposed to the uniformly red cold classicals, which all formed in the distant solar system (Fraser & Brown 2012). A hypothesis to explain the color bifurcation of objects formed at different heliocentric distances relies on the heliocentric-distance-dependent fractionation of surface volatiles with different sublimation temperatures (Brown et al. 2011). Sparser and lower-quality albedo data from *Spitzer* have been analyzed to reveal hints of a trend of increasing albedo with spectral slope for Centaurs (Stansberry et al. 2008), while a more intricate principal component analysis of TNO albedos and colors identifies 10 different groupings, 5 of which are red and compatible with the bright red type, 3 are dark and consistent with dark neutral surfaces, and the remaining 2 account for the largest bodies (Dalle Ore et al. 2013). Our analysis, using a significantly larger sample of high-quality albedos, builds on the trends above (e.g., our albedo-color clusters closely match the color bifurcation first seen in Fraser & Brown 2012) and, importantly, corroborates the idea that dynamical classes believed to originate beyond ~ 30 AU appear uniquely linked by a special combination of red color and high albedo.

The potentially unique surfaces of TNOs formed in-situ promise to shed light on some open questions. For instance, attempts to separate classical TNOs into hot and cold based on inclination and color thresholds have produced inconsistent results (Peixinho et al. 2008). Clearly, the two components are mixed, concealing the intrinsic inclination distribution of the locally formed cold population. Careful analysis of the orbits of bright red hot classicals may help separate the two populations in a more robust fashion. Another example is whether the scattered disk is being replenished from other excited dynamical classes, or if it is a fossil from the planetary instability epoch (Duncan & Levison 1997). We find that the distribution of scattered TNOs in color-albedo space is unlike that of Plutinos or hot classicals (significance level 98%, 2D Kolmogorov–Smirnov test) which naively suggests that the scattered disk is not being replenished from those populations. This is not unexpected from dynamical

arguments, but highlights the power of the surface type trends reported here. A detailed analysis of these questions, including the effects of object size, is beyond the scope of this Letter and will be the subject of a future paper.

No dynamical family in the outer solar system is composed solely of dark neutral objects. By contrast, objects closer to the Sun are composed entirely of dark, neutrally colored objects (Figure 4). JFCs, which are an end-state of the Centaurs, and Oort Cloud comets all have dark neutral surfaces. The same is true for inactive objects in cometary orbits, which are believed to be dead or dormant comets, and for Jupiter Trojans (Fornasier et al. 2007). The satellites of the giant planets have neutrally colored surfaces, but some of the largest moons have larger albedos. The lack of bright red surfaces among inner and intermediate solar system objects could be explained in two ways. Either these populations contain no bodies formed in the outer solar system, or the bright red material found on some TNOs is destroyed as they approach the Sun (Jewitt 2002). The fact that bright red surfaces are seen in some Centaurs but not in JFCs provides strong evidence in favor of the latter.

We report here on evidence from albedo and color data that TNOs native to the distant solar system ($\gtrsim 30$ AU) possess unique bright red surfaces, suggesting that a compositional discontinuity was in place before the solar system was dynamically mixed. One important caveat should be mentioned: the absence of dark neutral objects in our samples of cold classicals, outer resonants and detached TNOs may be caused by the combination of their lower albedo (hence larger size for the same magnitude) and the steep TNO size distribution. The current best estimates of the TNO luminosity function suggest that the higher albedo bright red objects are ~ 3 times more likely to be included in our sample than dark neutral objects (Fraser et al. 2014). For instance, the probability of drawing no dark neutral objects in a sample of 12 outer resonants, assuming they are intrinsically outnumbered 3 to 1, follows a binomial distribution and amounts to $p = 0.032$. It is thus possible that our sampling has missed objects that are nevertheless present. We note, however, that the dynamical classes in our sample composed solely of bright red objects taken as a whole (29 objects) lower the aforementioned probability to $p = 2.4 \times 10^{-4}$, beyond the typical 3σ threshold. Interestingly, an independent study of the colors of resonant TNOs finds cases of neutral surfaces in the 2:1 MMR (Sheppard 2012). These objects are not in our sample and lack albedo data, but could be consistent with the dark neutral group, which we do not see in the outer resonances.

Our data are unable to decide whether the entire bulk composition of planetesimals accreted at different locations varied as lower condensation temperature volatiles became available, or only the surface chemical makeup was modulated by the different sublimation temperature of various volatiles. For that, we may need flyby data on Centaurs and TNOs of both surface types and in-situ chemical sampling of comet nuclei to come from missions such as New Horizons and *Rosetta*.

5. CONCLUSIONS

We have analyzed the surface albedos and colors for a sample of 109 TNOs. The albedo data were obtained as part of the *Herschel* “TNOs Are Cool” survey of the outer solar system. Our main findings are as follows.

1. The surfaces of most TNOs fall into one of two types: dark neutral surfaces with albedos ~ 0.05 and spectral slopes $S \sim 10\%$, and bright red surfaces with higher albedos

~ 0.15 and significantly steeper spectral slopes $S \sim 35\%$. This clustering of surfaces lends support to the previously reported bifurcation in the colors of small, excited Kuiper Belt objects and Centaurs and highlights the importance of albedo data for the understanding of the surface properties of small solar system bodies.

- Importantly, we find that all TNOs in our sample thought to have formed and remained in the outer solar system possess bright red surfaces. These include the cold classical Kuiper Belt objects, the detached objects, and resonant TNOs in the 2:1 MMR with Neptune and beyond. We note, however, that the steep TNO size distribution may result in our small sample missing darker objects in these populations.

P.L. acknowledges support from the Michael West Fellowship and the Royal Society Newton Fellowship. Part of this work was supported by the German *DLR* project No. 50 OR 1108. R.D. acknowledges support from MINECO for his Ramón y Cajal Contract. C.K. was supported by the Hungarian Research Fund (OTKA) grant K-104607 and by the Bolyai Research Fellowship of the H.A.S.

Facility: Herschel

REFERENCES

- Batygin, K., Brown, M. E., & Fraser, W. C. 2011, *ApJ*, 738, 13
- Bauer, J. M., Grav, T., Blauvelt, E., et al. 2013, *ApJ*, 773, 22
- Brown, M. E., Schaller, E. L., & Fraser, W. C. 2011, *ApJL*, 739, L60
- Dalle Ore, C. M., Dalle Ore, L. V., Roush, T. L., et al. 2013, *Icar*, 222, 307
- Duncan, M. J., & Levison, H. F. 1997, *Sci*, 276, 1670
- Efron, B., & Tibshirani, R. J. 1993, *An Introduction to the Bootstrap*, Vol. 57 (Berlin: Springer)
- Fornasier, S., Barucci, M. A., de Bergh, C., et al. 2009, *A&A*, 508, 457
- Fornasier, S., Dotto, E., Hainaut, O., et al. 2007, *Icar*, 190, 622
- Fornasier, S., Lellouch, E., Müller, T., et al. 2013, *A&A*, 555, A15
- Fraser, W. C., & Brown, M. E. 2012, *ApJ*, 749, 33
- Fraser, W. C., Brown, M. E., Morbidelli, A., Parker, A., & Batygin, K. 2014, *ApJ*, 782, 100
- Gladman, B., Holman, M., Grav, T., et al. 2002, *Icar*, 157, 269
- Gladman, B., Marsden, B. G., & Vanlaerhoven, C. 2008, in *The Solar System Beyond Neptune*, ed. M. A. Barucci et al. (Tucson, AZ: Univ. Arizona Press), 43
- Gomes, R. S. 2003, *Icar*, 161, 404
- Hainaut, O. R., Boehnhardt, H., & Protopapa, S. 2012, *A&A*, 546, A115
- Jewitt, D. C. 2002, *AJ*, 123, 1039
- Kavelaars, J. J., Jones, R. L., Gladman, B. J., et al. 2009, *AJ*, 137, 4917
- Kiss, C., Müller, T. G., Vilenius, E., et al. 2013, *ExA*, 37, 161
- Lellouch, E., Kiss, C., Santos-Sanz, P., et al. 2010, *A&A*, 518, L147
- Lellouch, E., Santos-Sanz, P., Lacerda, P., et al. 2013, *A&A*, 557, A60
- Levison, H. F., & Morbidelli, A. 2003, *Natur*, 426, 419
- Levison, H. F., Morbidelli, A., Van Laerhoven, C., Gomes, R., & Tsiganis, K. 2008, *Icar*, 196, 258
- Levison, H. F., & Stern, S. A. 2001, *AJ*, 121, 1730
- Lim, T. L., Stansberry, J., Müller, T. G., et al. 2010, *A&A*, 518, L148
- Luu, J., & Jewitt, D. 1996, *AJ*, 112, 2310
- Luu, J. X., & Jewitt, D. C. 1990, *AJ*, 99, 1985
- Malhotra, R. 1995, *AJ*, 110, 420
- Mommert, M., Harris, A. W., Kiss, C., et al. 2012, *A&A*, 541, A93
- Morbidelli, A., Emel'yanenko, V. V., & Levison, H. F. 2004, *MNRAS*, 355, 935
- Morbidelli, A., Gaspar, H. S., & Nesvorný, D. 2014, *Icar*, 232, 81
- Müller, T. G., Lellouch, E., Bönhardt, H., et al. 2009, *EM&P*, 105, 209
- Müller, T. G., Lellouch, E., Stansberry, J., et al. 2010, *A&A*, 518, L146
- Pál, A., Kiss, C., Müller, T. G., et al. 2012, *A&A*, 541, L6
- Parker, A. H., & Kavelaars, J. J. 2010, *ApJL*, 722, L204
- Peixinho, N., Delsanti, A., Guilbert-Lepoutre, A., Gafeira, R., & Lacerda, P. 2012, *A&A*, 546, A86
- Peixinho, N., Doressoundiram, A., Delsanti, A., et al. 2003, *A&A*, 410, L29
- Peixinho, N., Lacerda, P., & Jewitt, D. 2008, *AJ*, 136, 1837
- Perna, D., Dotto, E., Barucci, M. A., et al. 2013, *A&A*, 554, A49
- Petit, J.-M., Kavelaars, J. J., Gladman, B. J., et al. 2011, *AJ*, 142, 131
- Santos-Sanz, P., Lellouch, E., Fornasier, S., et al. 2012, *A&A*, 541, A92
- Sheppard, S. S. 2012, *AJ*, 144, 169
- Stansberry, J., Grundy, W., Brown, M., et al. 2008, in *The Solar System Beyond Neptune*, ed. M. A. Barucci, H. Boehnhardt, D. P. Cruikshank, & A. Morbidelli (Tucson, AZ: Univ. Arizona Press), 161
- Stephens, D. C., & Noll, K. S. 2006, *AJ*, 131, 1142
- Tegler, S. C., & Romanishin, W. 2000, *Natur*, 407, 979
- Tibshirani, R., Walther, G., & Hastie, T. 2001, *J. R. Stat. Soc.: B (Stat. Methodol.)*, 63, 411
- Trujillo, C. A., & Sheppard, S. S. 2014, *Natur*, 507, 471
- Tsiganis, K., Gomes, R., Morbidelli, A., & Levison, H. F. 2005, *Natur*, 435, 459
- Vilenius, E., Kiss, C., Mommert, M., et al. 2012, *A&A*, 541, A94
- Vilenius, E., Kiss, C., Müller, T., et al. 2014, *A&A*, 564, A35
- Volk, K., & Malhotra, R. 2008, *ApJ*, 687, 714